JOINT INSTITUTE FOR NUCLEAR RESEARCH

Bogoliubov Laboratory of Theoretical Physics (BLTP)

FINAL REPORT ON THE INTEREST PROGRAMME

Numerical simulations for phase dynamics in Josephson nanojunctions

Supervisor:

Dr. Majed Nashaat.

Student:

Ahmed Eltohamy, Egypt
Alexandria university

Participation period:

October 30 – December 10, Wave 9

Abstract

In this practice I have learned how to simulate the current voltage characteristics for single Josephson junctions at different dissipation parameters. And record the voltage dynamics at different current values. In this part I used the resistively and capacitively shunted Josephson junctions (RCSJ) model to find the voltage across the junction.

The second part was devoted to micromagnetic simulations. Here, I studied the Landau–Lifshitz–Gilbert equation which describes the magnetic moment dynamics. And I got some experience for how to use Ubermag package to calculate magnetic hysteresis for thin film magnetic material for different anisotropic constant, and exchange interaction.

Contents

1. Josephson junction simulation:

1.1. Introduction

1.1.1. Josephson effect:

Brian D. Josephson predicted the Josephson effect in 1962, and it is just as significant as flux quantization.[1]

1.1.2. Short Josephson junction:

Superconductivity finds several uses in electronics, sensors, and high-frequency devices, thanks to the Josephson effect. When two superconductors are electrically coupled in a weak way, the Josephson effect is seen. There are numerous ways to develop this kind of communication [2].

Superconductor-insulator-superconductor (SIS) connections were the only ones considered in Josephson's original theoretical research.

The main principle of the short Josephson junction is the overlapping of the wave functions ($\psi_1 \; and \; \psi_2$) of the electrons of the $S_1 \; and \; S_2$ respectively[3]:

$$\psi_1 = \sqrt{n_s^{*1}}\, e^{i\theta_1} \quad (1.1)$$

$$\psi_2 = \sqrt{n_s^{*2}}\, e^{i\theta_2} \quad (1.2)$$

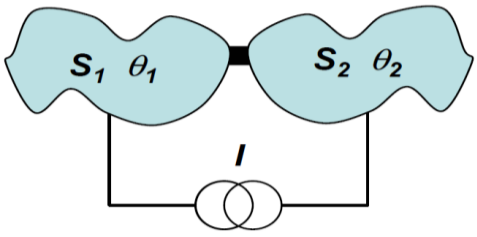

Fig. 1 Josephson junction (SIS) [3]

1.1.3. Lumped junctions

Lumped junctions are Josephson junctions that have a phase difference and a spatially uniform supercurrent density. A supercurrent can be used to characterize such junctions:

$$I_s = \int_S J_s . ds \quad (1.3)$$

Where J_s is the supercurrent density while the junction area S is the integration region. It is possible to rewrite the current-phase relation in terms of the currents as:

$$I_s = I_c \sin \phi(t) \quad (1.4)$$

where $I_s \; and \; I_c$ are the super and critical currents respectively.

The gauge-invariant phase difference is still given by:

$$\phi(t) = \theta_2(t) - \theta_1(t) - \frac{2\pi}{\Phi_0}\int_1^2 A(r,t).dl \qquad (1.5)$$

Where ϕ is the phase difference and the integral term represent the integration of the vector potential along (dl) (the distance between the two points which $\theta_1 \; and \; \theta_2$) were calculated.

Because the electric field at a lumped junction is independent of both y and z, it should be noted that the voltage is constant across the junction area, which extends for example, across the yz-plane. After then, the voltage-phase relation becomes:

$$\frac{d\phi}{dt} = \frac{2\pi}{\Phi_0} V \quad (1.6)$$

1.1.4.London equations:

The time derivative and the curvature of the supercurrent density expression are used to derive the phenomenological London equations. In its simplified form, they are provided with by:

$$\frac{\partial}{\partial t}(\Lambda J_s) = E \qquad (1.7) \; (1^{st} \text{ London equation})$$

$$\nabla \times (\Lambda J_s) = -B \quad (1.8) \; (2^{nd} \text{ London equation})$$

(Where, $\Lambda = \mu_0(\lambda_L)^2$ is London parameter and λ_L is London penetration depth.)

The gauge invariant phase difference j varies in time as (2^{nd} Josephson equation) in the presence of a finite potential difference $\Delta\mu \; = \; eV$ between the two superconductors.

$$\frac{d\phi}{dt} = \frac{2\pi}{\Phi_0} V = \frac{2eV}{\hbar} \qquad (1.9)$$

The Josephson current then oscillates in time as $I_s \; = \; I_c \; sin(\omega t \; + \phi_0)$

at a frequency $= \frac{\omega}{2\pi}$.

1.2. Modeling:

the equivalent circuit for SIS junction is:

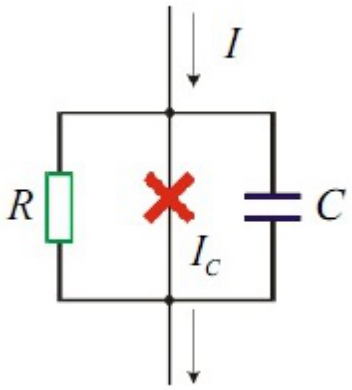

(RCSJ) (resistive-capacitive shunted junction)

(RCSJ) (Resistively Capacitively Shunted Junction)

The total current in the circuit is given by:

$$I_{total} = I_{disp} + I_{qp} + I_s \qquad (1.10)$$

where,

$I_{disp} = C\frac{dV}{dt}$ (displacement current)

$I_{qp} = \frac{V}{R}$ (quasi particle current)

$I_s = I_c \sin\phi$ (superconductor current)

$$I_{total} = C\frac{dV}{dt} + \frac{V}{R} + I_c \sin\phi \qquad (1.11)$$

where, C is the capacity of the capacitor, R is the resistance of the resistor I_C is the critical current and from equation (1.9) $V = \frac{\hbar}{2e}\frac{\partial\phi}{\partial t}$

Normalization of the system equation was done by using the following parameters:

$$V_0 = \frac{\hbar\omega_p}{2e}; \qquad \tau = \omega_p t; \qquad \omega_p = \sqrt{\frac{2eI_c}{C\hbar}}; \qquad \beta = \frac{1}{R}\sqrt{\frac{\hbar}{2eI_cC}};$$

$$\frac{I}{I_c} \to I \qquad \frac{V}{V_0} \to V$$

where, β is the dissipation parameter.

If we applied an external radiation, a radiation current term ($I_{Rad} = Asin(\omega t)$) is added. Where A is the amplitude and ω is the angular frequency.

$$\begin{cases} \dfrac{\partial\phi}{\partial t} = V \\ \dfrac{dV}{dt} = I - \sin\phi - \beta\dfrac{\partial\phi}{\partial t} \end{cases}$$

This system is solved by fourth order Runge–Kutta method by using a C++ code provided by the supervisor.

1.3. Results:

1.3.1. The I-V characteristic curves and the effect of β.

- **For ($\beta < 1$) (underdamped case):**

As the current increases the voltage jumps to a higher value when the current reaches the critical value. And hysteresis appears while the current is decreasing from the maximum value due to the capacitance of the junction as shown in the (fig.1(a)). We also noticed that as β increases the resistance decreases.

- **For $\beta > 1$ (overdamped case):**

Hysteresis disappeared due to neglecting the effect of the junction capacitance. So, by increasing and decreasing current, the IV-curve for both current directions will be the same as shown in the (Fig.1(b)).

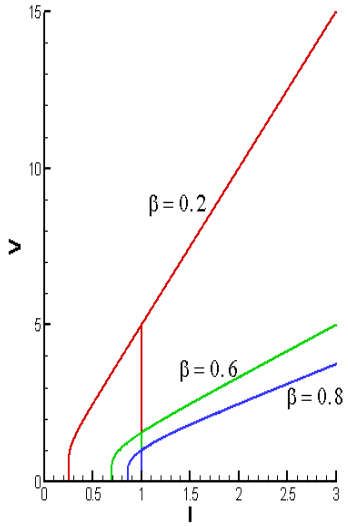

Fig.1(a): the effect of β on I_V characteristic curve at the underdamped case

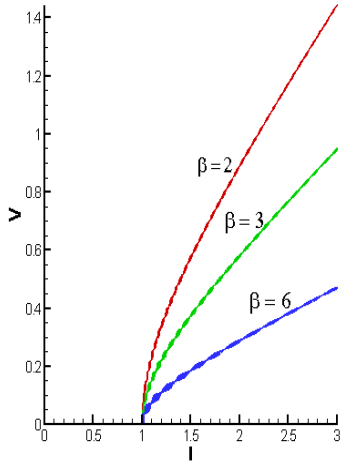

Fig.1 (b): the effect of β on I_V characteristic curve at the overdamped case

1.3.2. Time dependence characteristic curve and effect of β:

In this section, we investigate voltage time dependance at different bias current, and dissipation parameter.

- **For ($\beta < 1$) underdamped case**

The time dependence for voltage showed that while the current is less than critical current, the voltage zero (see Fig.2(a)) for I =0.5 and 0.7). When the current exceeds the critical value ($I \geq I_c$) the voltage appears (see Fig.2(a) for I = 1.5). For

($I < I_c$) the time dependance for voltage at I = 0.5 and 0.7 does not equal zero due to appearance of the hysteresis region.

- **For ($\beta > 1$) Overdamped case:**

In this case as we have seen in I-V characteristic curve, the voltage takes the same path while the current is increasing or decreasing as s shown in (Fig.2 (b)), the voltage has a value only at ($I \geq I_c$).

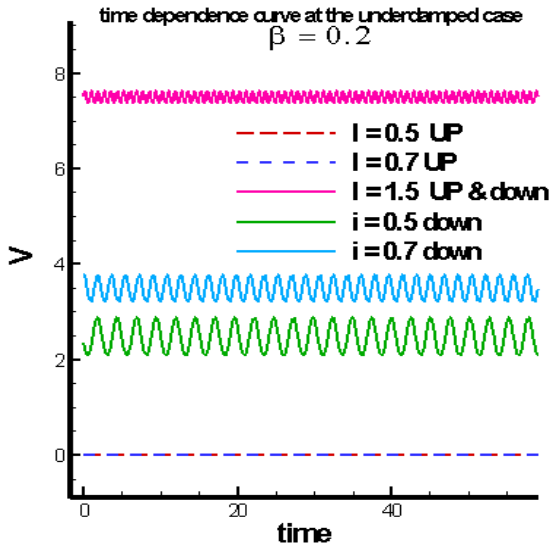

Fig.2(a) Voltage Time dependence curve at the under damped case

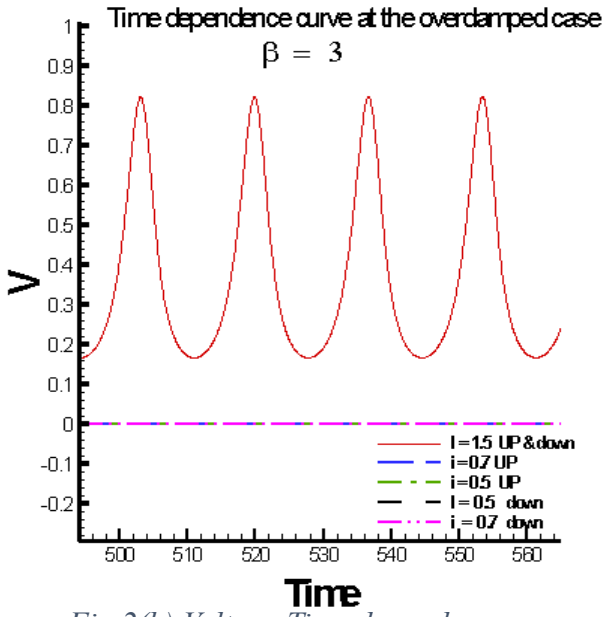

Fig.2(b) Voltage Time dependence curve at the Overdamped case

- **Effect of external radiation**

In this section we have studied the effect of radiation on the voltage behavior. If we apply an external ac current or voltage source, a constant voltage step appears in the IV- characteristics due the phase of the junction locks to the drive frequency and this is known as Shapiro steps which appear at quantized values of voltage, their width has a Bessel function dependence on the amplitude V_1 of the ac voltage.

- **Overdamped case:**

Shapiro steps appears at values of voltage equals to*:*

$$V_n = n\,\omega$$

where ω *is the angular frequency the applied radiation.* Where $n = 1,2,3, \ldots \ldots$ as shown in (Fig 3 (a)) and (Fig.3 (b)).

The width of the DC intervals is proportional to the amplitude of the current spike according to the following equation:

$$\Delta I = I_c J_n \left(\frac{2\pi V_1}{\Phi_0 \omega}\right)$$

- **<u>Underdamped case:</u>**

In this case Shapiro steps appear at fractional values of voltage as shown in (Fig.3(C)).

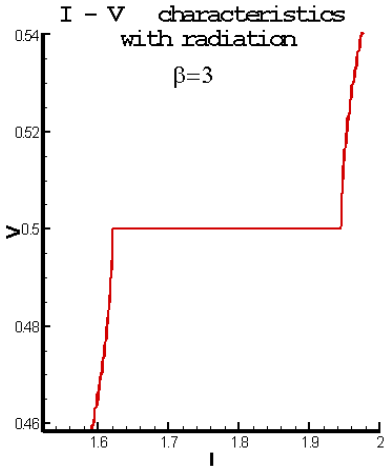

Fig.3(a) Shapiro step at overdamped case at $V_n = 1\,\omega$

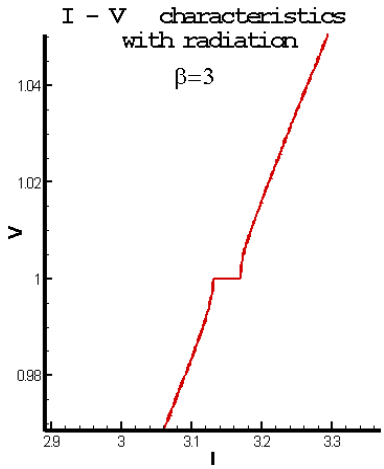

Fig.3(b) Shapiro step at overdamped case at $V_n = 2\omega$

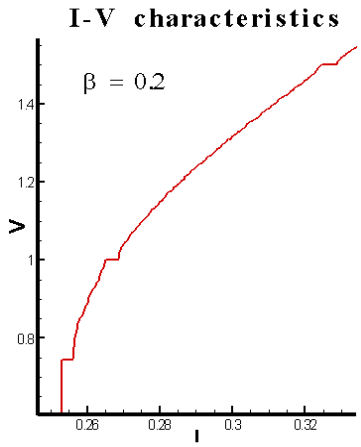

Fig.3(C) Shapiro steps at underdamped case

2. Micromagnetic simulation:

In this part, we investigate the magnetic hysteresis for ferromagnetic material at different magnetic energy parameters.

2.1. Dynamics equation:

The dynamics of magnetization field m, without external excitations (e.g. spin-polarized current) is governed by the Landau-Lifshitz-Gilbert (LLG) equation [4,5].

$$\frac{dm}{dt} = -\gamma_0(m \times H_{rff}) + \alpha\left(m \times \frac{dm}{dt}\right)$$

where $\gamma_0 = \mu_0\gamma$ is the gyromagnetic ratio, α is the Gilbert damping, and $H_{eff} = -\frac{1}{\mu_0 M_s}\frac{\delta w(m)}{\delta m}$ is the effective field. It consists of two terms: precession and damping. In this tutorial, we will explore some basic properties of this equation to understand how to define it in simulations.

2.2. Energy equation:

Any magnetic system is exposed to a group of energies that are produced by the interaction if the magnetic moment of the electrons with each other and with the external applied magnetic field. And these energies are.

2.2.1. Zeeman energy:

This is energy due to the external applied magnetic field.

$$E_z = -\mu_0 M_s m.H$$

where, μ_0 & M_s are the magnetic permeability and saturation magnetization respectively.

2.2.2. Exchange energy:

The energy due to the interaction between the neighboring electrons

$$E_{ex} = A_{ex}(\nabla m)^2$$

where A_{ex} is the exchange energy parameter.

2.2.3. Uniaxial anisotropy energy:

This energy term explained that each part of the system can have individual energy.

$E_a = -K(m.u)$ where, u is the easy axis direction.

where, K is the uniaxial anisotropy energy parameter.

2.2.4. Dzyaloshinskii-Moriya energy:

While the exchange interaction aims to align (neighboring) magnetic moments parallel to each other, the Dzyaloshinskii-Moriya (DM) energy wants to align them perpendicular to each other.

$$E_d m = D[m_z \nabla . m - (m . \nabla) m_z]$$

where, D is the Dzyaloshinskii-Moriya energy parameter.

So, the total energy equation becomes:

$$E_{system} = \int (-\mu_0 M_s m . H) + (A(\nabla m)^2) + (-K(m . u) + (D[m_z \nabla . m - (m . \nabla) m_z])) \, dV$$

2.3. Ubermag simulation:

The simulation is done by Ubermag simulator using (oommfc) as a magnetic calculator.

The simulation is done on a cell with dimensions (50nm,50nm,50nm) and the mesh was (5nm,5nm,5nm). And the applied magnetic field was $8 \times 10^6 A/m$ in Z direction, and the (y-component) of the magnetization was studied giving us the following results.

2.4. Results

When the external applied magnetic field is removed, the magnetic moment doesn't return to the initial state and the hysteresis area appeared.

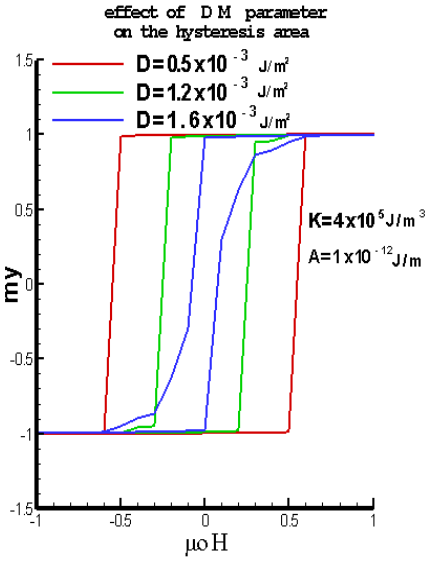

Fig (4) (a) the effect of DM parameter on the hysteresis area

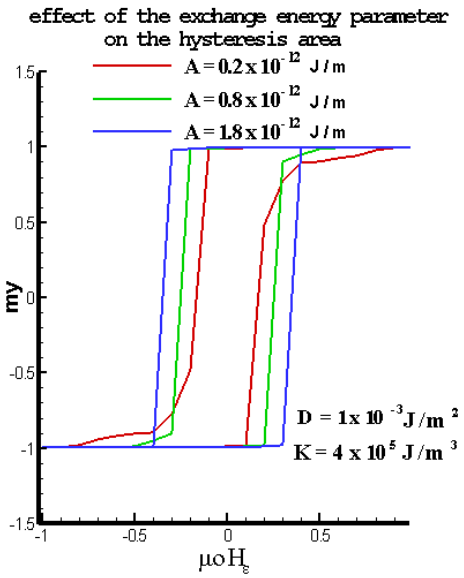

Fig (4) (b) the effect of exchange energy parameter on the hysteresis area

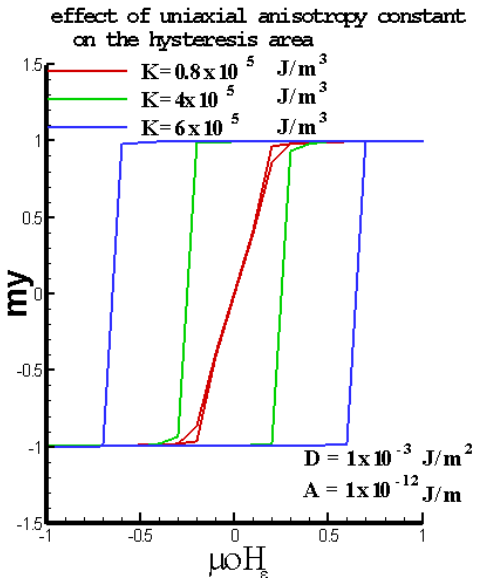

Fig (4) (c) the effect of uniaxial anisotropy energy parameter on the hysteresis area

By studying the magnetization at different values of the energy parameters, we found that, as (DM) increases the hysteresis area decreases and when (A_{ex} and K) increase the hysteresis area increases.

3. Conclusion

In this practice I have studied the behavior of the current and the voltage of short Josephson junction. And I have seen the effect of the dissipation parameter β. When $\beta > 1$ (overdamping case) as the current increases, the voltage is zero for current below the critical current. If the current exceeds the critical current, the voltage appears across the junction. By increasing β the resistance of the junction decreases. While as $\beta < 1$ (underdamping case) in which as the current increases, the voltage is zero when the current is below the critical current. When the current exceeds the critical current, the voltage appears but, in this case when the current decreasing the hysteresis appears because of the junction capacitance and the voltage appears at the hysteresis area. Also, we have studied the effect of the applied external radiation with angular frequency (ω) on the junction which leads to appearance of Shapiro steps due to that the junction locks to the drive frequency and this is known as Shapiro step which appears at quantized values of voltage.

Then, we studied the micromagnetic system and the effect of the energy parameters (A_{ex} , D and K) on magnetization hysteresis we found that, as D increases the hysteresis area decreases and when (A_{ex} and K) increase the hysteresis area increases.

4. References:

1. 28Brian D. Josephson, Possible new effects in superconductive tunnelling, Phys. Lett. 1, 251–253 (1962).

2. K. K. Likharev. Superconducting weak links. Reviews of Modern Physics, 51(1):101, 1979.

3. Prof. Dr. Rudolf Gross & Dr. Achim Marx, Applied Superconductivity: Josephson Effect and Superconducting Electronics, October 2005.

4. L.D. Landau, E.M. Lifshitz, Theory of the dispersion of magnetic permeability in ferromagnetic bodies. Phys. Z. Sowietunion 8, 153 (1935)

5. T.L. Gilbert, Physical Review, 100 (1955), p. 1243.